

CONTENTS

The effect of oxidation on fatigue crack growth in 2.25Cr-1Mo steel at 525 °C: A metallographic examination	1
K. D. Challenger (Monterey, CA, U.S.A.), R. P. Skelton (Surrey, U.K.) and J. S. Kamen (Monterey, CA, U.S.A.)	
Probabilistic aspects of the strength of fiber-dominated short-fiber composites I: Aligned fibers	7
R. C. Wetherhold (Buffalo, NY, U.S.A.)	
Probabilistic aspects of the strength of fiber-dominated short-fiber composites II: Biased fiber distribution	13
R. C. Wetherhold (Buffalo, NY, U.S.A.)	
Fracture mechanisms in Cu-O and Cu-Pb alloys fatigued with a positive mean stress	19
R. Eckert, C. Laird and J. L. Bassani (Philadelphia, PA, U.S.A.)	
Effect of the welding process and heat input on the fracture toughness of welded joints in high strength low alloy steel	29
P. Sundaram, R. K. Pandey and A. N. Kumar (New Delhi, India)	
Influence of the martensite content on the fatigue behaviour of a dual-phase steel	39
W. Zhongguang, W. Guonan, K. Wei and H. Haicai (Shenyang, China)	
The effect of anisotropy on creep and creep crack growth in cold-worked C-Mn steel at 360 °C	45
D. J. Gooch (Surrey, U.K.)	
Crystallographic texture, anisotropic yield surfaces and forming limits of sheet metals	55
F. Barlat (Alcoa Center, PA, U.S.A.)	
Low cycle fatigue behaviour of a cryogenic Fe-30Mn-5Al-0.1Nb-0.3C steel	73
J. K. Han and Y. G. Kim (Seoul, South Korea)	
Mechanism of fracture produced by fatigue cycling with a positive mean stress in copper	81
R. Eckert, C. Laird and J. Bassani (Philadelphia, PA, U.S.A.)	
Corrosion behavior of sensitized austenitic (AISI 304) stainless steel in a CO ₂ atmosphere	89
S. K. Putatunda (Detroit, MI, U.S.A.)	
Effect of the nitrogen-to-hydrogen ratio on the mechanical behavior of vanadium, niobium and tantalum . .	97
W. A. Spitzig and C. V. Owen (Ames, IA, U.S.A.)	
The effect of aging on the yield stress of a single-crystal superalloy	105
A. A. Hopgood and J. W. Martin (Oxford, U.K.)	
The dislocation structure in beryllium single-crystals deformed by prismatic slip	111
S. Jönsson and J. Beuers (Stuttgart, F.R.G.)	
Fatigue crack initiation and propagation in AISI 4130 steel exposed to neutral perchlorate solution	125
Z. Y. Zhu, G. C. Farrington and C. Laird (Philadelphia, PA, U.S.A.)	
Influence of dynamic strain aging on the creep ductility of solid solution alloys	137
S. I. Hong (Philadelphia, PA, U.S.A.)	
Plastic deformation in B.C.C. alloys induced by hydrogen concentration gradients	143
M. E. Armacanqui and R. A. Oriani (Minneapolis, MN, U.S.A.)	
The generation of thermal stress and strain during the quenching of steel plates in polyalkylene glycol . .	153
A. J. Fletcher and A. B. Soomro (Sheffield, U.K.)	
Transmission electron microscopy studies of the dislocation microstructures in fatigued Fe-8.7Al-29.7Mn-1.04C alloy	161
S. C. Tjong and N. J. Ho (Kaohsiung, Taiwan)	
A comprehensive analysis of the static indentation process	169
Y. Tirupataiah and G. Sundararajan (Hyderabad, India)	
Low temperature magnetic properties of F.C.C. Fe-Cr-Ni alloys:	
Effects of manganese and interstitial carbon and nitrogen	181
E. R. Jones, Jr., T. Datta, C. Almasan, D. Edwards (Columbia, SC, U.S.A.) and H. M. Ledbetter (Boulder, CO, U.S.A.)	
An investigation of phase transformation in a 50.8at.%Ni-Ti shape memory alloy	189
L. Zuemin and T. Y. Hsu (Xu Zuyao) (Shanghai, China)	
Thermal contraction stresses in cemented tungsten carbide composites	195
C. M. Sayers (Bath, U.K.)	

(continued on inside back cover)

CONTENTS (continued)

Microstructural characterization of rapidly solidified aluminium-transition metal alloys	201
J. M. Sater, S. C. Jha and T. H. Sanders, Jr. (West Lafayette, IN, U.S.A.)	
On the transition from a waveless to a wavy interface in explosive welding	217
D. Jaramillo, V. A. Azecket and O. T. Inal (Socorro, NM, U.S.A.)	
Effects of molybdenum, titanium and silicon additions on the $D0_3 \rightleftharpoons B2$ transition temperature for alloys near Fe_3Al	223
R. T. Fortnum and D. E. Mikkola (Houghton, MI, U.S.A.)	
Dissolution of comminuted magnesium oxide as affected by the density of dislocations introduced by various comminution methods	233
N. F. Albanese-Kotar and D. E. Mikkola (Houghton, MI, U.S.A.)	
Dissolution of comminuted magnesium oxide as affected by the density of dislocations introduced by various comminution methods	233
N. F. Albanese-Kotar and D. E. Mikkola (Houghton, MI, U.S.A.)	
Elemental analysis of Swedish nuclear waste glasses:	
Leachability vs. composition	241
D. E. Clark (Gainesville, FL, U.S.A.), A. Lodding, H. Odellius (Gothenburg, Sweden) and L. O. Werme (Stockholm, Sweden)	
The erosion of Abresist	257
M. K. Aghajamian, E. Breval, J. S. Jennings and N. H. MacMillan (University Park, PA, U.S.A.)	
BOOK REVIEWS	265
CONFERENCE CALENDAR	269
LETTERS	
Auger electron spectroscopy of anodic oxide films on nickel-copper alloys	L1
R. D. K. Misra (Hyderabad, India)	
Estimation of monocrystal elastic constants for an alloy of a cubisolvant and an hexagonal solute	L5
D. J. B. Cohen and Y. M. Koo (Evanston, IL, U.S.A.)	
Plasma-induced erosion of monocrystalline alloy surfaces	L9
M. Rubel (Stockholm, Sweden)	
Plasma sprayed superconducting oxides	L13
R. A. Neiser (Stony Brook, NY, and Landover, MD, U.S.A.), J. P. Kirkland (Landover, MD, U.S.A.), H. Herman (Stony Brook, NY, U.S.A.), W. T. Elam and E. F. Skelton (Washington, DC, U.S.A.)	
AUTHOR INDEX	275
SUBJECT INDEX	277

© ELSEVIER SEQUOIA S.A. (1987)

0025-5416/87/\$3.50

All rights reserved. No part of this publication may be reproduced, stored in a retrieval system or transmitted in any form or by any means, electronic, mechanical, photocopying, recording or otherwise, without the prior written permission of the publisher, Elsevier Sequoia S.A., P.O. Box 851, 1007 Lausanne 1, Switzerland.

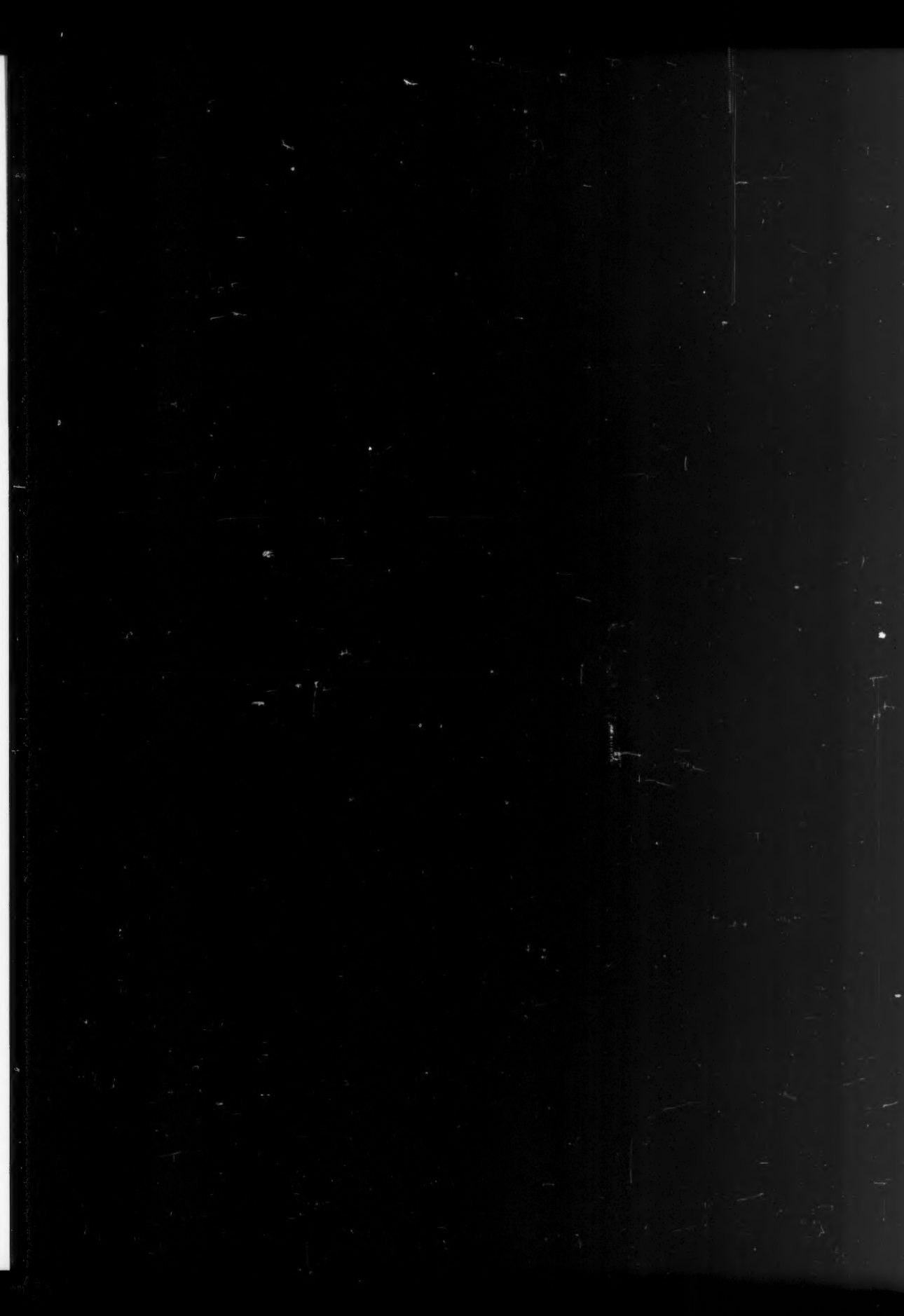
Submission of an article for publication implies the transfer of the copyright from the author(s) to the publisher and entails the author(s) irrevocable and exclusive authorization of the publisher to collect any sums or considerations for copying or reproduction payable by third parties.

Upon acceptance of an article by the journal, the author(s) will be asked to transfer copyright of the article to the publisher. This transfer will ensure the widest possible dissemination of information.

For Material Subject to U.S. Copyright Law

Special regulations for readers in the U.S.A.

This journal has been registered with the Copyright Clearance Center, Inc., 21 Congress Street, Salem, MA 01970, U.S.A. Consent is given for copying of articles for personal use, or for the personal use of specific clients. This consent is given on the condition that the copier pays through the Center the per-copy fee stated in the code on the first page of each article for copying beyond that permitted by Sections 107 or 108 of the U.S. Copyright Law. If no code appears in an article, the author has not given broad consent to copy and permission to copy must be obtained directly from the author. All articles published prior to 1981 may be copied for a per-copy fee of U.S. \$2.50, also payable through the Center. This consent does not extend to other kinds of copying, such as for general distribution, resale, advertising and promotion purposes or for creating new collective works. Special written permission must be obtained from the publisher for such copying.





Author Index

- Aghajamian, M. K., 257
 Albanese-Kotar, N. F., 233
 Almasan, C., 181
 Armacanqui, M. E., 143
 Barlat, F., 55
 Bassani, J. L., 19, 81
 Beuers, J., 111
 Breval, E., 257
 Challenger, K. D., 1
 Clark, D. E., 241
 Cohen, J. B., L5
 Datta, T., 181
 Eckert, R., 19, 81
 Edwards, D., 181
 Elam, W. T., L13
 Farrington, G. C., 125
 Fletcher, A. J., 153
 Fortnum, R. T., 223
 Gooch, D. J., 45
 Guonan, W., 39
 Haicai, H., 39
 Han, J. K., 73
 Herman, H., L13
 Ho, N. J., 161
 Hong, S. I., 137
 Hopgood, A. A., 105
 Hsu, T. Y., (Xu Zuyao), 189
 Inal, O. T., 217
 Jaramillo, D., 217
 Jennings, J. S., 257
 Jha, S. C., 201
 Jones, Jr., E. R., 181
 Jönsson, S., 111
 Kamen, J. S., 1
 Kim, Y. G., 73
 Kirkland, J. P., L13
 Koo, Y. M., L5
 Kumar, A. N., 29
 Laird, C., 19, 81, 125
 Ledbetter, H. M., 181
 Lodding, A., 241
 MacMillan, N. H., 257
 Martin, J. W., 105
 Mikkola, D. E., 223, 233
 Misra, R. D. K., L1
 Neiser, R. A., L13
 Odelius, H., 241
 Oriani, R. A., 143
 Owen, C. V., 97
 Pandey, R. K., 29
 Putatunda, S. K., 89
 Rubel, M., L9
 Sanders, Jr., T. H., 201
 Sater, J. M., 201
 Sayers, C. M., 195
 Skelton, E. F., L13
 Skelton, R. P., 1
 Soomro, A. B., 153
 Spitzig, W. A., 97
 Sundaram, P., 29
 Sundararajan, G., 169
 Szecket, V. A., 217
 Tirupataiah, Y., 169
 Tjong, S. C., 161
 Wei, K., 39
 Werme, L. O., 241
 Wetherhold, R. C., 7, 13
 Xuemin, L., 189
 Zhongguang, W., 39
 Zhu, Z. Y., 125



Subject Index

- Abresist**
erosion of Abresist, 257
- Aging**
effect of aging on the yield stress of a single-crystal superalloy, 105
influence of dynamic strain aging on the creep ductility of solid solution alloys, 137
- AISI 4130 steel**
fatigue crack initiation and propagation in AISI 4130 steel exposed to neutral perchlorate solution, 125
- Alloys**
Auger electron spectroscopy of anodic oxide films on nickel-copper alloys, L1
effects of molybdenum, titanium and silicon additions on the $DO_3 \rightleftharpoons B2$ transition temperature for alloys near Fe_3Al , 223
effect of the welding process and heat input on the fracture toughness of welded joints in high strength low alloy steel, 29
estimation of monocrystal elastic constants for an alloy of a cubic solvent and an hexagonal solute, L5
fracture mechanisms in Cu-O and Cu-Pb alloys fatigued with a positive mean stress, 19
influence of dynamic strain aging on the creep ductility of solid solution alloys, 137
investigation of phase transformation in a 50.8 at.%Ni-Ti shape memory alloy, 189
low temperature magnetic properties of F.C.C. Fe-Cr-Ni alloys: effects of manganese and interstitial carbon and nitrogen, 181
microstructural characterization of rapidly solidified aluminium-transition metal alloys, 201
plasma-induced erosion of monocrystalline alloy surfaces, L9
plastic deformation in B.C.C. alloys induced by hydrogen concentration gradients, 143
transmission electron microscopy studies of the dislocation microstructures in fatigued Fe-8.7Al-29.7Mn-1.04C alloy, 161
- Aluminium**
low cycle fatigue behaviour of a cryogenic Fe-30Mn-5Al-0.1Nb-0.3C steel, 73
microstructural characterization of rapidly solidified aluminium-transition metal alloys, 201
transmission electron microscopy studies of the dislocation microstructures in fatigued Fe-8.7Al-29.7Mn-1.04C alloy, 161
- Anisotropic yield surfaces**
crystallographic texture, anisotropic yield surfaces and forming limits of sheet metals, 55
- Anisotropy**
effect of anisotropy on creep and creep crack growth in cold-worked C-Mn steel at 360 °C, 45
- Auger electron spectroscopy**
Auger electron spectroscopy of anodic oxide films on nickel-copper alloys, L1
- Austenitic (AISI 304) stainless steel**
corrosion behavior of sensitized austenitic (AISI 304) stainless steel in a CO_2 atmosphere, 89
- B.C.C. alloys**
plastic deformation in B.C.C. alloys induced by hydrogen concentration gradients, 143
- Beryllium**
dislocation structure in beryllium single-crystals deformed by prismatic slip, 111
- Biased fiber distribution**
probabilistic aspects of the strength of fiber-dominated short-fiber composites II: biased fiber distribution, 13
- Carbon**
effect of anisotropy on creep and creep crack growth in cold-worked C-Mn steel at 360 °C, 45
low temperature magnetic properties of F.C.C. Fe-Cr-Ni alloys: effects of manganese and interstitial carbon and nitrogen, 181
transmission electron microscopy studies of the dislocation microstructures in fatigued Fe-8.7Al-29.7Mn-1.04C alloy, 161
- Carbon dioxide**
corrosion behavior of sensitized austenitic (AISI 304) stainless steel in a CO_2 atmosphere, 89
- Chromium**
effect of oxidation on fatigue crack growth in 2.25Cr-1Mo steel at 525 °C: a metallographic examination, 1
- low temperature magnetic properties of F.C.C. Fe-Cr-Ni alloys: effects of manganese and interstitial carbon and nitrogen, 181**
- Cold-worked C-Mn steel**
effect of anisotropy on creep and creep crack growth in cold-worked C-Mn steel at 360 °C, 45
- Comminuted magnesium oxide**
dissolution of comminuted magnesium oxide as affected by the density of dislocations introduced by various comminution methods, 233
- Composites**
probabilistic aspects of the strength of fiber-dominated short-fiber composites I: aligned fibers, 7
probabilistic aspects of the strength of fiber-dominated short-fiber composites II: biased fiber distribution, 13
thermal contraction stresses in cemented tungsten carbide composites, 195

- Composition**
- elemental analysis of Swedish nuclear waste glasses: leachability *vs.* composition, 241
- Copper**
- Auger electron spectroscopy of anodic oxide films on nickel-copper alloys, L1
 - fracture mechanisms in Cu-O and Cu-Pb alloys fatigued with positive mean stress, 19
 - mechanism of fracture produced by fatigue cycling with a positive mean stress in copper, 81
- Corrosion behavior**
- corrosion behavior of sensitized austenitic (AISI 304) stainless steel in a CO₂ atmosphere, 89
- Crack**
- effect of anisotropy on creep and creep crack growth in cold-worked C-Mn steel at 360 °C, 45
 - effect of oxidation on fatigue crack growth in 2.25Cr-1Mo steel at 525 °C: a metallographic examination, 1
 - fatigue crack initiation and propagation in AISI 4130 steel exposed to neutral perchlorate solution, 125
- Creep**
- effect of anisotropy on creep and creep crack growth in cold-worked C-Mn steel at 360 °C, 45
 - influence of dynamic strain aging on the creep ductility of solid solution alloys, 137
- Cryogenic Fe-20Mn-5Al-0.1Nb-0.3C steel**
- low cycle fatigue behaviour of a cryogenic Fe-30Mn-5Al-0.1Nb-0.3C steel, 73
- Crystallographic**
- crystallographic texture, anisotropic yield surfaces and forming limits of sheet metals, 55
- Crystals**
- dislocation structure in beryllium single-crystals deformed by prismatic slip, 111
- Cubic solvent**
- estimation of monocrystal elastic constants for an alloy of a cubic solvent and an hexagonal solute, L5
- Deformation**
- plastic deformation in B.C.C. alloys induced by hydrogen concentration gradients, 143
- Dislocation**
- dislocation structure in beryllium single-crystals deformed by prismatic slip, 111
 - dissolution of comminuted magnesium oxide as affected by the density of dislocations introduced by various comminution methods, 233
 - transmission electron microscopy studies of the dislocation microstructures in fatigued Fe-8.7Al-29.7Mn-1.04C alloy, 161
- Dissolution**
- dissolution of comminuted magnesium oxide as affected by the density of dislocations introduced by various comminution methods, 233
- Double-phase steel**
- influence of the martensite content on the fatigue behaviour of a dual-phase steel, 39
- Dynamic strain aging**
- influence of dynamic strain aging on the creep ductility of solid solution alloys, 137
- Elemental analysis**
- elemental analysis of Swedish nuclear waste glasses: leachability *vs.* composition, 241
- Erosion**
- erosion of Abresist, 257
 - plasma-induced erosion of monocrystalline alloy surfaces, L9
- Explosive welding**
- transition from a waveless to a wavy interface in explosive welding, 217
- Fatigue**
- fatigue crack initiation and propagation in AISI 4130 steel exposed to neutral perchlorate solution, 125
 - influence of the martensite content on the fatigue behaviour of a dual-phase steel, 39
 - low cycle fatigue behaviour of a cryogenic Fe-30Mn-5Al-0.1Nb-0.3C steel, 73
- Fatigue crack growth**
- effect of oxidation on fatigue crack growth in 2.25Cr-1Mo steel at 525 °C: a metallographic examination, 1
- Fatigue cycling**
- mechanism of fracture produced by fatigue cycling with a positive mean stress in copper, 81
- F.C.C. Fe-Cr-Ni alloys**
- low temperature magnetic properties of F.C.C. Fe-Cr-Ni alloys: effects of manganese and interstitial carbon and nitrogen, 181
- Fibers**
- probabilistic aspects of the strength of fiber-dominated short-fiber composites I: aligned fibers, 7
- Fiber-dominated short-fiber composites**
- probabilistic aspects of the strength of fiber-dominated short-fiber composites I: aligned fibers, 7
 - probabilistic aspects of the strength of fiber-dominated short-fiber composites II: biased fiber distribution, 13
- Films**
- Auger electron spectroscopy of anodic oxide films on nickel-copper alloys, L1
- Fracture**
- mechanism of fracture produced by fatigue cycling with a positive mean stress in copper, 81
- Fracture mechanisms**
- fracture mechanisms in Cu-O and Cu-Pb alloys fatigued with a positive mean stress, 19
- Fracture toughness**
- effect of the welding process and heat input on the fracture toughness of welded joints in high strength low alloy steel, 29
- Glasses**
- elemental analysis of Swedish nuclear waste glasses: leachability *vs.* composition, 241

- Hexagonal solute**
 estimation of monocrystal elastic constants for an alloy of a cubic solvent and an hexagonal solute, L5
- Hydrogen**
 plastic deformation in B.C.C. alloys induced by hydrogen concentration gradients, 143
- Indentation**
 comprehensive analysis of the static indentation process, 169
- Iron**
 low cycle fatigue behaviour of a cryogenic Fe-30Mn-5Al-0.1Nb-0.3C steel, 73
 low temperature magnetic properties of F.C.C. Fe-Cr-Ni alloys: effects of manganese and interstitial carbon and nitrogen, 181
 transmission electron microscopy studies of the dislocation microstructures in fatigued Fe-8.7Al-29.7Mn-1.04C alloy, 161
- Iron aluminide**
 effects of molybdenum, titanium and silicon additions on the $\text{DO}_3 \rightleftharpoons \text{B}2$ transition temperature for alloys near Fe_3Al , 223
- Joints**
 effect of the welding process and heat input on the fracture toughness of welded joints in high strength low alloy steel, 29
- Leachability**
 elemental analysis of Swedish nuclear waste glasses: leachability vs. composition, 241
- Lead**
 fracture mechanisms in Cu-O and Cu-Pb alloys fatigued with a positive mean stress, 19
- Magnesium oxide**
 dissolution of comminuted magnesium oxide as affected by the density of dislocations introduced by various comminution methods, 233
- Magnetic properties**
 low temperature magnetic properties of F.C.C. Fe-Cr-Ni alloys: effects of manganese and interstitial carbon and nitrogen, 181
- Manganese**
 effect of anisotropy on creep and creep crack growth in cold-worked C-Mn steel at 360 °C, 45
 low cycle fatigue behaviour of a cryogenic Fe-30Mn-5Al-0.1Nb-0.3C steel, 73
 low temperature magnetic properties of F.C.C. Fe-Cr-Ni alloys: effects of manganese and interstitial carbon and nitrogen, 181
 transmission electron microscopy studies of the dislocation microstructures in fatigued Fe-8.7Al-29.7Mn-1.04C alloy, 161
- Martensite**
 influence of the martensite content on the fatigue behaviour of a dual-phase steel, 39
- Mechanical behavior**
 effect of the nitrogen-to-hydrogen ratio on the mechanical behavior of vanadium, niobium and tantalum, 97
- Metallographic examination**
 effect of oxidation on fatigue crack growth in 2.25Cr-1Mo steel at 525 °C: a metallographic examination, 1
- Metals**
 crystallographic texture, anisotropic yield surfaces and forming limits of sheet metals, 55
- Microstructural characterization**
 microstructural characterization of rapidly solidified aluminium-transition metal alloys, 201
- Microstructures**
 transmission electron microscopy studies of the dislocation microstructures in fatigued Fe-8.7Al-29.7Mn-1.04C alloy, 161
- Molybdenum**
 effects of molybdenum, titanium and silicon additions on the $\text{DO}_3 \rightleftharpoons \text{B}2$ transition temperature for alloys near Fe_3Al , 223
 effect of oxidation on fatigue crack growth in 2.25Cr-1Mo steel at 525 °C: a metallographic examination, 1
- Monocrystal elastic constants**
 estimation of monocrystal elastic constants for an alloy of a cubic solvent and an hexagonal solute, L5
- Monocrystalline alloy surfaces**
 plasma-induced erosion of monocrystalline alloy surfaces, L9
- Nickel**
 Auger electron spectroscopy of anodic oxide films on nickel-copper alloys, L1
 investigation of phase transformation in a 50.8-at.%Ni-Ti shape memory alloy, 189
 low temperature magnetic properties of F.C.C. Fe-Cr-Ni alloys: effects of manganese and interstitial carbon and nitrogen, 181
- Niobium**
 effect of the nitrogen-to-hydrogen ratio on the mechanical behavior of vanadium, niobium and tantalum, 97
 low cycle fatigue behaviour of a cryogenic Fe-30Mn-5Al-0.1Nb-0.3C steel, 73
- Nitrogen**
 low temperature magnetic properties of F.C.C. Fe-Cr-Ni alloys: effects of manganese and interstitial carbon and nitrogen, 181
- Nitrogen-to-hydrogen**
 effect of the nitrogen-to-hydrogen ratio on the mechanical behavior of vanadium, niobium and tantalum, 97
- Nuclear waste glasses**
 elemental analysis of Swedish nuclear waste glasses: leachability vs. composition, 241
- Oxidation**
 effect of oxidation on fatigue crack growth in 2.25Cr-1Mo steel at 525 °C: a metallographic examination, 1
- Oxides**
 plasma sprayed superconducting oxides, L13
- Oxygen**
 fracture mechanisms in Cu-O and Cu-Pb alloys fatigued with a positive mean stress, 19

- Perchlorate**
 fatigue crack initiation and propagation in AISI 4130 steel exposed to neutral perchlorate solution, 125
- Phase transformation**
 investigation of phase transformation in a 50.8 at.-%Ni-Ti shape memory alloy, 189
- Plasma-induced erosion**
 plasma-induced erosion of monocrystalline alloy surfaces, L9
- Plasma sprayed superconducting oxides**, L13
- Plastic**
 plastic deformation in B.C.C. alloys induced by hydrogen concentration gradients, 143
- Polyalkylene glycol**
 generation of thermal stress and strain during the quenching of steel plates in polyalkylene glycol, 153
- Prismatic slip**
 the dislocation structure in beryllium single-crystals deformed by prismatic slip, 111
- Quenching**
 generation of thermal stress and strain during the quenching of steel plates in polyalkylene glycol, 153
- Steels**
 corrosion behavior of sensitized austenitic (AISI 304) stainless steel in a CO₂ atmosphere, 89
 effect of anisotropy on creep and creep crack growth in cold-worked C-Mn steel at 360 °C, 45
 effect of oxidation on fatigue crack growth in 2.25Cr-1Mo steel at 525 °C: a metallographic examination, 1
 effect of the welding process and heat input on the fracture toughness of welded joints in high strength low alloy steel, 29
 generation of thermal stress and strain during the quenching of steel plates in polyalkylene glycol, 153
 influence of the martensite content on the fatigue behaviour of a dual-phase steel, 39
 low cycle fatigue behaviour of a cryogenic Fe-30Mn-5Al-0.1Nb-0.3C steel, 73
- Sheet metals**
 crystallographic texture, anisotropic yield surfaces and forming limits of sheet metals, 55
- Silicon**
 effects of molybdenum, titanium and silicon additions on the DO₃ ⇌ B2 transition temperature for alloys near Fe₃Al, 223
- Single-crystal superalloy**
 effect of aging on the yield stress of a single-crystal superalloy, 105
- Slip**
 dislocation structure in beryllium single-crystals deformed by prismatic slip, 111
- Solid solution alloys**
 influence of dynamic strain aging on the creep ductility of solid solution alloys, 137
- Solidified aluminium-transition metal alloys**
 microstructural characterization of rapidly solidified aluminium-transition metal alloys, 201
- Solvent**
 estimation of monocrystal elastic constants for an alloy of a cubic solvent and an hexagonal solute, L5
- Static indentation process**
 comprehensive analysis of the static indentation process, 169
- Strain**
 generation of thermal stress and strain during the quenching of steel plates in polyalkylene glycol, 153
- Strength**
 probabilistic aspects of the strength of fiber-dominated short-fiber composites I: aligned fibers, 7
 probabilistic aspects of the strength of fiber-dominated short-fiber composites II: biased fiber distribution, 13
- Stress**
 effect of aging on the yield stress of a single-crystal superalloy, 105
 fracture mechanisms in Cu-O and Cu-Pb alloys fatigued with a positive mean stress, 19
 generation of thermal stress and strain during the quenching of steel plates in polyalkylene glycol, 153
 mechanism of fracture produced by fatigue cycling with a positive mean stress in copper, 81
- Stresses**
 thermal contraction stresses in cemented tungsten carbide composites, 195
- Superconducting oxides**
 plasma sprayed superconducting oxides, L13
- Surfaces**
 crystallographic texture, anisotropic yield surfaces and forming limits of sheet metals, 55
 plasma-induced erosion of monocrystalline alloy surfaces, L9
- Tantalum**
 effect of the nitrogen-to-hydrogen ratio on the mechanical behavior of vanadium, niobium and tantalum, 97
- Thermal contraction stresses**
 thermal contraction stresses in cemented tungsten carbide composites, 195
- Thermal stress**
 generation of thermal stress and strain during the quenching of steel plates in polyalkylene glycol, 153
- Titanium**
 effects of molybdenum, titanium and silicon additions on the DO₃ ⇌ B2 transition temperature for alloys near Fe₃Al, 223
 investigation of phase transformation in a 50.8 at.-%Ni-Ti shape memory alloy, 189
- Transition**
 transition from a waveless to a wavy interface in explosive welding, 217
- Transition metal**
 microstructural characterization of rapidly solidified aluminium-transition metal alloys, 201
- Transmission electron microscopy**
 transmission electron microscopy studies of the dislocation microstructures in fatigued Fe-8.7Al-29.7Mn-1.04C alloy, 161

Transition temperature

effects of molybdenum, titanium and silicon additions on the $\text{DO}_3 \rightleftharpoons \text{B}2$ transition temperature for alloys near Fe_3Al , 223

Tungsten carbide

thermal contraction stresses in cemented tungsten carbide composites, 195

Vanadium

effect of the nitrogen-to-hydrogen ratio on the mechanical behavior of vanadium, niobium and tantalum, 97

Waveless interface

transition from a waveless to a wavy interface in explosive welding, 217

Wavy interface

transition from a waveless to a wavy interface in explosive welding, 217

Welding

effect of the welding process and heat input on the fracture toughness of welded joints in high strength low alloy steel, 29

transition from a waveless to a wavy interface in explosive welding, 217